Design and parameter tuning of a robust model predictive controller for UAVs

Nathan Michel [*,**] **Sylvain Bertrand** [*] **Giorgio Valmorbida** [**]
Sorin Olaru [**] **Didier Dumur** [**]

[*] *ONERA - The French Aerospace Lab, F-91123 Palaiseau, France (e-mail: nathan.michel@onera.fr ; sylvain.bertrand@onera.fr)*
[**] *L2S, CentraleSupélec, CNRS, Univ. Paris-Sud, Université Paris-Saclay, 3 rue Joliot-Curie, Gif-Sur-Yvette 91192, France (e-mail: giorgio.valmorbida@l2s.centralesupelec.fr ; sorin.olaru@l2s.centralesupelec.fr ; didier.dumur@centralesupelec.fr)*

Abstract: Two formulations of robust model predictive control (MPC) that have robustness properties with respect to bounded additive disturbance over conventional MPC are applied to Unmanned Aerial Vehicle (UAV) translational dynamics. These controllers use results from invariant sets theory. The tuning of the proposed MPC laws is studied, and their performances are compared in simulations.

Keywords: Robust MPC, UAV, bounded additive disturbance, polytope, parameters tuning

1. INTRODUCTION

The last decade has witnessed a significant increase in the number of tasks performed by Unmanned Aerial Vehicles (UAVs). Among these we can cite commercial tasks such as goods delivery (Mo et al. (2016)), terrain mapping (Tahar et al. (2011)) and building inspection (Choi and Kim (2015)). The design of controllers enabling UAVs to perform autonomously such tasks should take into account safety and technological constraints, such as distance to obstacles or actuator limitations. Moreover, UAVs are subject to disturbances, such as ground effect or aerodynamic perturbations when flying close to obstacles (McKinnon (2015)).

Previous works have been carried out on robust control of UAVs, from a switching model strategy (Alexis et al. (2011)) to a robust PID controller (Kada and Ghazzawi (2011)). These strategies are designed to guarantee robustness with respect to bounded disturbances, but do not take constraints into account.

In this context, constraint handling in the control law design can benefit from MPC strategies. Also, the ability to cope with bounded disturbances on the system dynamics has been extensively studied and current MPC strategies allow for improved robustness and stability properties (Scokaert and Mayne (1998) Langson et al. (2004)).

One possible robustification of an MPC strategy consists in computing a trajectory for a disturbance free version of the system by a classical MPC, while simultaneously making use of an additional control law to maintain the state of the perturbed system inside a "tube" around the nominal trajectory (Langson et al. (2004)). This method requires an a priori knowledge on the disturbance bounds affecting the system. These strategies have been extensively studied for linear systems (Mayne et al. (2006) Mayne et al. (2005)). The problem of position stabilization of a UAV in presence of constraints and disturbances can fit into this framework.

The MPC strategies in this study are based on invariant sets (Blanchini (1999)) using existing methods (Olaru et al. (2010)). Stability is guaranteed by making use of a terminal stabilizing constraint (Mayne et al. (2000)), defined by sets whose construction is detailed. The tuning of two linear robust MPC controllers (Mayne et al. (2005)) and a comparison of their performances are studied with simulations. The disturbance model used in simulations is based on experimental results (McKinnon (2015)).

This paper is structured as follows. In Section 2, the equations of motion of a quadrotor UAV are introduced while results on invariant sets and related properties are presented in Section 3. In Section 4, two robust MPC controllers are described, and their tuning is studied in Section 5. Simulation results are presented in Section 6.

Notation Given two sets $X \in \mathbb{R}^n$ and $Y \in \mathbb{R}^n$, the Minkowski sum and Pontryagin difference are defined as

$$X \oplus Y = \{x + y | x \in X, y \in Y\},$$
$$X \ominus Y = \{x | x \oplus Y \subset X\}$$

For two vectors $x \in \mathbb{R}^3$ and $y \in \mathbb{R}^3$, the cross product is denoted $x \times y$.
A polytope $P \subset \mathbb{R}^n$ is described as the convex-hull of a finite set of points $\{v_1, v_2, ..., v_{n_v}\}$

$$P = \{x | x = \sum_{i=1}^{n_v} \lambda_i v_i, \sum_{i=1}^{n_v} \lambda_i = 1\}$$

or as the set of solutions to a system of linear inequalities

$$P = \{x | A(P)x + b(P) \leq 0\}$$

with $A(P) \in \mathbb{R}^{p \times n}, b(P) \in \mathbb{R}^p$ and $p \in \mathbb{N}$.
The i^{th} power of a matrix A is denoted A^i.
The eigenvalues set of a matrix A is denoted $\lambda(A)$.

2. UAV MODELING

Consider an inertial frame $\mathbb{I} = (O, i, j, k)$ and a body frame $\mathbb{B}$ attached to the vehicle, the UAV equations of motion are

$$\dot{\xi} = v, \tag{1}$$
$$m\dot{v} = -mgk + RF + F_{ext}, \tag{2}$$
$$\dot{R} = RQ(\omega), \tag{3}$$
$$J\dot{\omega} = -\omega \times J\omega + \tau, \tag{4}$$

where $\xi = (p_x, p_y, p_z)^\top$ is the position of the center of gravity of the quadrotor in $\mathbb{I}$, $v = (v_x, v_y, v_z)^\top$ its velocity in $\mathbb{I}$, m its mass, $R \in SO(3)$ the orientation matrix, $\omega = (\omega_x, \omega_y, \omega_z)^\top$ its angular velocity in the body frame, J its inertia matrix, g the gravity constant, and

$$Q(\omega) = \begin{pmatrix} 0 & -\omega_z & \omega_y \\ \omega_z & 0 & -\omega_x \\ -\omega_y & \omega_x & 0 \end{pmatrix}.$$

The resulting force and torque generated by the quadrotor propellers are denoted F and τ and are expressed in the body frame $\mathbb{B}$, F_{ext} represents forces in the inertial frame due to external disturbances.
Define

$$u = -gk + R_{ref}F_{ref}/m$$

yielding

$$\dot{v} = u + ((RF - R_{ref}F_{ref}) + F_{ext})/m. \tag{5}$$

We assume that a control law defining the torque τ is given and guarantees a fast convergence of the entries of the orientation matrix R to a reference value R_{ref}. The motors dynamics are also neglected, thus F is assumed to converge instantaneously to F_{ref}. These asumptions are accounted for in the definition of the bounds in the disturbance term.
The equations (1) and (5) thus correspond to a double integrator with bounded additive disturbance. We discretize this system with a zero-order hold on u with sampling-time δ_t to obtain

$$x[k+1] = Ax[k] + Bu[k] + w[k], \tag{6}$$

$$A = \begin{pmatrix} 1 & \delta_t & 0 & 0 & 0 & 0 \\ 0 & 1 & 0 & 0 & 0 & 0 \\ 0 & 0 & 1 & \delta_t & 0 & 0 \\ 0 & 0 & 0 & 1 & 0 & 0 \\ 0 & 0 & 0 & 0 & 1 & \delta_t \\ 0 & 0 & 0 & 0 & 0 & 1 \end{pmatrix}, B = \begin{pmatrix} \frac{\delta_t^2}{2} & \delta_t & 0 & 0 & 0 & 0 \\ 0 & 0 & \frac{\delta_t^2}{2} & \delta_t & 0 & 0 \\ 0 & 0 & 0 & 0 & \frac{\delta_t^2}{2} & \delta_t \end{pmatrix}^\top$$

where $x = (p_x, v_x, p_y, v_y, p_z, v_z)^\top$, and $w \in \mathbb{W}$ is a term related to the discretization of the term $1/m((R_{ref}F_{ref} - RF) + F_{ext})$. If u is bounded and if the attitude controller is stabilizing, it can be shown that the error term $R_{ref}F_{ref} - RF$ is also bounded. Since F_{ext} is assumed to be bounded too, the disturbance term w is bounded. This system (6) will be referred to as the *uncertain system*.
The following sections will present MPC strategies for the regulation of the uncertain system (i.e. the UAV translational motion).

3. INVARIANT SETS AND FEEDBACK POLICY

The spatial and control constraints are defined by $x \in \mathbb{X} \subset \mathbb{R}^6$ and $u \in \mathbb{U} \subset \mathbb{R}^3$, with $\mathbb{X}$ and $\mathbb{U}$ bounded polytopes containing the origin in their interior. We assume $\mathbb{W}$ is a polytopic set containing the origin and such that $w \in W$. Denote the disturbance-free system

$$\bar{x}[k+1] = A\bar{x}[k] + B\bar{u}[k]. \tag{7}$$

This system is called the *nominal system*. Let us consider the following control policy for the uncertain system

$$u[k] = \bar{u}[k] + K(x[k] - \bar{x}[k]), \tag{8}$$

with $K \in \mathbb{R}^{3\times 6}$ such that $A_K = A + BK$ is Schur. The error $z[k] = x[k] - \bar{x}[k]$ verifies

$$z[k+1] = A_K z[k] + w[k]. \tag{9}$$

Definition 1. (Blanchini (1999)) The set Z is said robustly positively invariant (RPI) for the system (9) if for all $z[k] \in Z$ and all $w[k] \in \mathbb{W}$, $z[k+1] \in Z$.
The following proposition states that the control policy (8) ensures that the error remains in a RPI set Z.

Proposition 1. (Mayne et al. (2005), p.221) Suppose Z is RPI for $z[k+1] = A_K z[k] + w[k]$. Assume that $x[k] \in \{\bar{x}[k]\} \oplus Z$ and $u[k] = \bar{u}[k] + K(x[k] - \bar{x}[k])$, then $x[k+1] \in \{\bar{x}[k+1]\} \oplus Z$ for all $w[k] \in \mathbb{W}$.

Define the following sets

$$\bar{\mathbb{X}} = \mathbb{X} \ominus Z, \tag{10}$$
$$\bar{\mathbb{U}} = \mathbb{U} \ominus KZ. \tag{11}$$

If the nominal system satisfies the constraints ($\bar{x} \in \bar{\mathbb{X}}$ and $\bar{u} \in \bar{\mathbb{U}}$), then the uncertain system constraints are satisfied (i.e. $x \in \mathbb{X}$ and $u \in \mathbb{U}$).
Remark: the set containment $Z \subset \mathbb{X}$ and $KZ \subset \mathbb{U}$ have to hold to guarantee $\bar{\mathbb{X}} \neq \emptyset$ and $\bar{\mathbb{U}} \neq \emptyset$.

4. ROBUST MPC

4.1 Robust model predictive controller

This section presents the design of a nominal system control law using an MPC approach. Take an MPC algorithm given by the solution of the optimal control problem $P_N(\bar{x}[k])$ with the quadratic cost function

$$V_N(\bar{x}_0, \bar{\boldsymbol{u}}) = \sum_{i=0}^{N-1} (\bar{x}_i^\top Q\bar{x}_i + \bar{u}_i^\top P\bar{u}_i) + \bar{x}_N^\top Q_f \bar{x}_N. \tag{12}$$

The weighting matrices Q, P and Q_f are positive definite, N is the length of the prediction horizon. $P_N(\bar{x}[k])$ consists in minimizing $V_N(\bar{x}_0, \boldsymbol{u})$ with $\bar{x}_0 = \bar{x}[k]$. In this optimization problem, the control input sequence $\bar{\boldsymbol{u}} = \{\bar{u}_0, \bar{u}_1, ..., \bar{u}_{N-1}\}$ is the decision variable.

$$\begin{aligned} P_N(\bar{x}[k]) : & V_N^0(\bar{x}[k]) = min(V_N(\bar{x}_0, \bar{\boldsymbol{u}})), \\ & \bar{u}_i \in \bar{\mathbb{U}}, \forall i \in \{0, ..., N-1\}, \\ & \bar{x}_0 = \bar{x}[k], \\ & \bar{x}_i \in \bar{\mathbb{X}}, \forall i \in \{0, ..., N-1\}, \\ & \bar{x}_N \in \bar{\mathbb{X}}_f, \subset \bar{\mathbb{X}} \\ & \bar{x}_{i+1} = A\bar{x}_i + B\bar{u}_i, \forall i \in \{0, ..., N-1\}. \end{aligned}$$

The optimal control sequence is denoted $\bar{\boldsymbol{u}}^0$. The terminal weigth Q_f and the terminal set $\bar{\mathbb{X}}_f$ are defined to ensure stability.

Proposition 2. (Mayne et al. (2005), p.221) Let $K_f \in \mathbb{R}^{3\times 6}$ be a feedback gain matrix. Suppose K_f, Q_f and $\bar{\mathbb{X}}_f$ are such that:

$$
\begin{aligned}
&(A+BK_f)\bar{\mathbb{X}}_f \subset \bar{\mathbb{X}}_f,\\
&K_f\bar{\mathbb{X}}_f \subset \bar{\mathbb{U}}, \qquad (13)\\
&\bar{\mathbb{X}}_f \subset \bar{\mathbb{X}},\\
&((A+BK_f)\bar{x})^\top Q_f(A+BK_f)\bar{x} + (K_f\bar{x})^\top PK_f\bar{x},\\
&-\bar{x}^\top Q_f\bar{x} \leq 0, \forall \bar{x} \in \bar{\mathbb{X}}_f. \qquad (14)
\end{aligned}
$$

Then the origin is exponentially stable for the controlled nominal system (7) and recursive feasibility of the optimization problems is ensured.

Its feasibility domain is denoted $\bar{\mathbb{X}}_N$. Once the optimization problem $P_N(\bar{x}[k])$ is solved, the nominal control input $\bar{u}[k]$ is set as the first element of the optimal control input sequence $\bar{u}_0^0$. The next nominal state $\bar{x}[k+1]$ and the control input $u[k]$ are given by (7) and (8).
The successive optimization problems can be precomputed: they involve the nominal state only, which is not impacted by the disturbance sequence. It is therefore possible to compute beforehand the nominal system trajectory. The control input component $K(x[k]-\bar{x}[k])$, that ensures the uncertain system remains in a "tube" centered on this trajectory, is computed online.

4.2 Modified Robust MPC

The control input sequence $\bar{\boldsymbol{u}}$ is the decision variable of the optimization problem $P_N(\bar{x}[k])$ previously described. The modification presented here, as initially proposed in Mayne et al. (2005), consists in letting $\bar{x}_0 = \bar{x}[k]$ be a decision parameter. At each time step, the nominal state $\bar{x}[k]$ and the optimal control sequence $\bar{\boldsymbol{u}}^0$ are taken as the solution of the optimization problem $\check{P}_N(x[k])$:

$$
\begin{aligned}
\check{P}_N(x[k]) :& \check{V}_N^0(x[k]) = min(V_N(\bar{x}_0, \bar{\boldsymbol{u}})),\\
&\bar{u}_i \in \bar{\mathbb{U}}, \forall i \in \{0,...,N-1\},\\
&x[k] \in \{\bar{x}_0\} \oplus Z,\\
&\bar{x}_i \in \bar{\mathbb{X}}, \forall i \in \{0,...,N-1\},\\
&\bar{x}_N \in \bar{\mathbb{X}}_f \subset \bar{\mathbb{X}},\\
&\bar{x}_{i+1} = A\bar{x}_i + B\bar{u}_i, \forall i \in \{0,...,N-1\}.
\end{aligned}
$$

The optimal control sequence is denoted $\bar{\boldsymbol{u}}^0$ and the optimal initial state $\bar{x}_0^0$. The control input applied to the system is

$$u[k] = \bar{u}_0^0 + K(x[k] - \bar{x}_0^0).$$

Its feasibility domain is denoted $\mathbb{X}_N$. It can be proved that $\bar{\mathbb{X}}_N \oplus Z = \mathbb{X}_N$ (Mayne et al. (2005)). The conditions on Q_f and $\bar{\mathbb{X}}_f$ defined in Proposition 2 guarantee recursive feasibility and robust exponential stability of the set Z for the controlled uncertain system.
The successive optimization problems involved in this controller can not be solved offline, indeed, the disturbance $w[k]$ can not be forecast and it impacts the state $x[k+1]$. Therefore, the optimization problems have to be solved online.

Proposition 3. For all $x \in Z$, $\check{V}_N^0(x) = 0, \bar{x}_0^0 = 0, \bar{\boldsymbol{u}}^0 = \mathbf{0}$ and $u = \bar{u} + K(x - \bar{x}) = Kx$

Once the uncertain system has reached the RPI set Z, the optimization problem is trivial and Z is invariant for the uncertain system.

Both controllers presented in this section have robustness properties with regard to bounded additive disturbance. The tuning of their parameters is studied in the next section, and their closed loop performances are compared in Section 6.

5. TUNING PARAMETERS

The two controllers involve two sets of tuning parameters, (K, Z) and $(K_f, Q_f, \bar{\mathbb{X}}_f)$, the influence of which is analyzed below. The impact of the weighting matrices Q and P and of the prediction horizon length N of $P_N(\bar{x})$ and $\check{P}_N(x)$ are not detailed here.

5.1 Feedback gain K

The set Z defines the maximal error $z[k] = x[k] - \bar{x}[k]$ between the nominal and the uncertain state, and can be considered as the key element of the control law regarding the precision of the controlled system with respect to the disturbance $\mathbb{W}$. Moreover, it also defines the sets $\bar{\mathbb{X}}$ and $\bar{\mathbb{U}}$ of the optimization problems:

- a smaller set Z implies a larger set $\bar{\mathbb{X}} = \mathbb{X} - Z$.
- for a given feedback gain K, a smaller set Z implies a larger set $\bar{\mathbb{U}} = \mathbb{U} - KZ$.

For a given feedback gain K, it is possible to define the minimal Robust Positive Invariant (mRPI) set Z^* (Blanchini (1999))

$$Z^* = \bigoplus_{i=0}^{\infty} A_K^i W.$$

A feedback gain K leading to smaller eigenvalues of A_K will result in a smaller set Z^* and a larger set KZ^*.
The tuning of K impacts both the disturbance rejection and the constraints of the optimization problems.
Remark: In general, Z^* is not polytopic and cannot be explicitly characterized. Hence, the set Z is chosen as an RPI outer polytopic approximation of the mRPI Z^* (Olaru et al. (2010)).

5.2 Feedback gain K_f

For a given horizon length N, the admissible initial condition set $\bar{\mathbb{X}}_N$ is defined by the terminal constraint set $\bar{\mathbb{X}}_f$. This set is given by the following relations

$$
\begin{aligned}
&\bar{\mathbb{X}}_1 = \{\bar{x} \in \bar{\mathbb{X}} | \exists \bar{u} \in \bar{\mathbb{U}}, A\bar{x} + B\bar{u} \in \bar{\mathbb{X}}_f\},\\
&\bar{\mathbb{X}}_{i+1} = \{\bar{x} \in \bar{\mathbb{X}} | \exists \bar{u} \in \bar{\mathbb{U}}, A\bar{x} + B\bar{u} \in \bar{\mathbb{X}}_i\}, \forall i \leq 1.
\end{aligned}
$$

For given sets $(\bar{U}, \bar{\mathbb{X}})$, a larger set $\bar{\mathbb{X}}_f$ leads to a larger set $\bar{\mathbb{X}}_N$ of admissible initial conditions. The set $\bar{\mathbb{X}}_f$ has to verify (13). A smaller feedback gain K_f leads to a larger set $\bar{\mathbb{X}}_f$, hence to a larger set $\bar{\mathbb{X}}_N$.
Remark: Due to (14), the feedback gain K_f has an impact on the terminal cost $\bar{x}_N^\top Q_f \bar{x}_N$.

6. SIMULATIONS

Consider below the example related to a critical flight of a UAV close to a wall. The state constraints are $x \in \mathbb{X} = \{x | -5m \leq p_x \leq 5m, -0.5m \leq p_y \leq 1m, -0.2m \leq p_z \leq 1m, -1m.s^{-1} \leq v_x, v_y, v_z \leq 1m.s^{-1}\}$. The control input

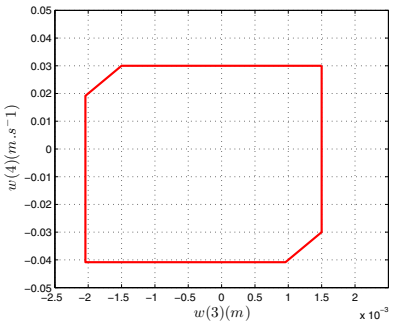

Fig. 1. Projection of the disturbance set on (p_y, v_y).

constraints are $u \in \mathbb{U} = \{u | -1m.s^{-2} \leq u_x, u_y, u_z \leq 1m.s^{-2}\}$. The structure of the above constraints are such that the three directions (p_x, v_x), (p_y, v_y) and (p_z, v_z) can be adressed independently. Hence, the 6 dimensional optimization problem is separated into 3 independent 2-dimensional optimization problems. In the following, the results will be presented for one direction. Similar results are obtained in the other two directions.

The sampling-time is $\delta_t = 0.1s$ and the horizon length $N = 15$. The weighting matrices Q and P are $Q = diag(10, 1)$ and $P = 0.1$. The disturbance w is modeled as the sum of two components

- the external force w_{ext} accounting for the discretization of the disturbance term F_{ext}/m due to the proximity of the system to a wall, whose value is taken from experimental data (McKinnon (2015)),
- a bounded term w_{ran} accounting for the discretization of the disturbance term $(R_{ref}F_{ref} - RF)/m$, whose value is randomly generated in a set $\mathbb{W}_{ran}$ at each time step

The projection of the set $\mathbb{W}$ is presented in Figure 1.

6.1 Feedback controller K

The feedback gain K is computed by using a pole placement strategy for the matrix A_K. The method presented in Olaru et al. (2010) defines, for a given feedback gain K, a sequence of RPI sets $\boldsymbol{Z} = (Z_0, Z_1, ...)$ such that $\forall i \in \mathbb{N}, Z_{i+1} \subset Z_i$. These sets are presented in Figure 2 for $\lambda(A + BK) = \{0.70, 0.60\}$. The iterations increase the complexity of the polytope (i.e. the number of vertices of its convex hull) while decreasing its area (Figure 2).
The 6^{th} iteration Z_6 is presented in Figure 3 for $\lambda(A + BK) = \{0.30, 0.20\}$, $\{0.70, 0.60\}$ and $\{0.90, 0.80\}$. The associated bounds on $\bar{u}$ are $|\bar{u}| \leq 0.34, 0.54$ and $0.59m.s^{-2}$. For a given $i \in \mathbb{N}$, placing poles closer to 0 tends to reduce the size of Z_i while increasing the size of KZ_i.

The simulation is run with $\lambda(A+BK) = \{0.70, 0.60\}$ and $Z = Z_6$.

6.2 Terminal constraints

The feedback gain K_f is computed using a pole placement strategy for the matrix $A + BK_f$. In this study, the algorithm used to compute the set $\bar{\mathbb{X}}_f$ is the following

- Initialization: $\Omega_0 = \{x \in \bar{\mathbb{X}} | K_f x \in \bar{\mathbb{U}}\}$,

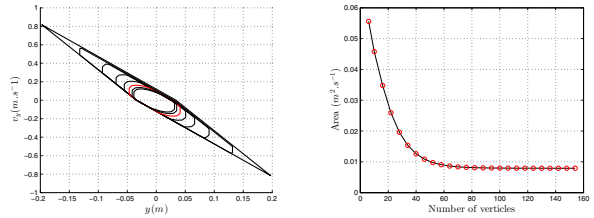

Fig. 2. (Left) Projection of the sets $Z_i, i = 0, ..., 8$ for $\lambda(A + BK) = \{0.70, 0.60\}$. (Right) Relation between the area of the iterations Z_i and their number of vertices $v(Z_i)$.

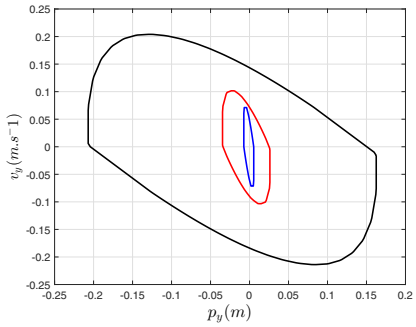

Fig. 3. Projection of the set Z_6 for $\lambda(A + BK) = \{0.30, 0.20\}$ (blue),$\lambda(A + BK) = \{0.70, 0.60\}$ (red) and $\lambda(A + BK) = \{0.90, 0.80\}$ (black).

.

- Iteration: $\Omega_{i+1} = \{x | A(\Omega_i)x + b(\Omega_i) \leq 0, A(\Omega_i)(A + BK_f)x + b(\Omega_i) \leq 0\}, \forall i \geq 0$.

The computation stops at the l^{th} iteration such that $\Omega_{l+1} = \Omega_l$, which implies $(A + BK_f)\Omega_l \subset \Omega_l$. Thus, the set Ω_l verifies the conditions of Proposition 2.
Finite time convergence of the algorithm is not guaranteed with the above strict stopping criterion. However, a relative convergence test can be used based on the decrease of the Hausdorff distance between consecutive iterations. It can be noted that the convergence speed increases for smaller eigenvalues of $A + BK_f$ which is relative to the contraction factor of the set mapping.

Figure 4 presents the sets $\bar{\mathbb{X}}_f$ and $\bar{\mathbb{X}}_N$ obtained for different sets of eigenvalues of $A + BK_f$. Closed-loop eigenvalues with absolute value close to 1 increase the size of the set of admissible initial conditions while increasing the complexity of the set $\bar{\mathbb{X}}_f$, that defines constraints in the optimization problem.
The simulation is run with $\lambda(A + BK_f) = \{0.95, 0.90\}$.

6.3 Controller performance comparison

The two controllers presented in Sections 4.1 and 4.2 have been simulated with the same initial conditions $x[0] = (0.5, 0, 0.5, 0, 0.5, 0)^\top$ and random disturbance sequence. The stabilization problem consists in steering the state of the system to the reference chosen to be the origin. The closed-loop evolution of p_y are illustrated in Figure 5, and the control input in Figure 6.
The control input is closer to the bounds of $\mathbb{U}$ ($|u_y| = 1m.s^{-2}$) for controller 2. This is due to the fact that $x - \bar{x}$ takes extremal values in Z for controller 2 (Figure 7).

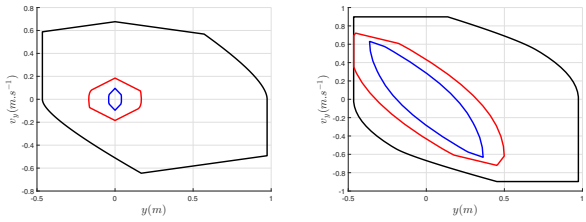

Fig. 4. Projection of the sets $\bar{\mathbb{X}}_f$ (left) and $\bar{\mathbb{X}}_N$ (right) on (p_y, v_y) for $\lambda(A + BK_f) = \{0.97, 0.95\}$ (black), $\lambda(A + BK_f) = \{0.90, 0.80\}$ (red) and $\lambda(A + BK_f) = \{0.80, 0.60\}$ (blue).

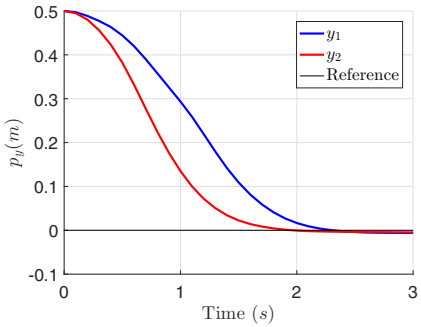

Fig. 5. Time evolution of p_y for controller 1 (blue) and controller 2 (red).

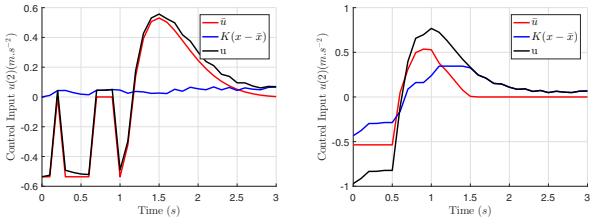

Fig. 6. Time evolution of the control inputs u, $\bar{u}$ and $K(x-\bar{x})$ with controller 1 (left) and controller 2 (right).

Moreover, Figure 6 illustrates that $\bar{u}$ and $K(x - \bar{x})$ have the same sign until $\bar{u} = 0$ (i.e. once the uncertain system has reached the set Z as mentioned in Proposition 3). This version allows the "tube" control input $K(x - \bar{x})$ to not only reject disturbance but also to contribute in steering the state of the uncertain system to the reference.

In both simulations, the state of the uncertain system x remains in the "tube" $\bar{x} \oplus Z$ as illustrated in Figure 7.

7. CONCLUSION

We have presented the computation of the sets involved in the robust model predictive controllers developed in Mayne et al. (2005) for a simplified UAV model. The tuning parameters of those MPC controllers and their impact on both the system performance and the optimization problem have been studied. Two robust model predictive controllers have been compared with simulations, using disturbance models from McKinnon (2015).

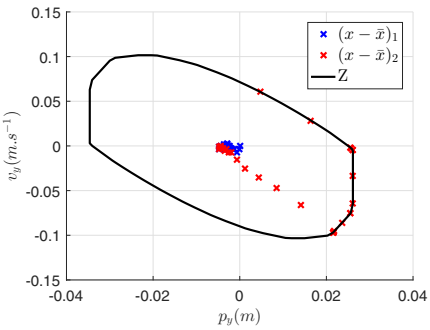

Fig. 7. Projection on the plane (p_y, v_y) of the difference $x - \bar{x}$ with controller 1 (blue) and controller 2 (red).

REFERENCES

Alexis, K., Nikolakopoulos, G., and Tzes, A. (2011). Switching model predictive attitude control for a quadrotor helicopter subject to atmospheric disturbances. *Control Engineering Practice*, 19(10), 1195 – 1207.

Blanchini, F. (1999). Set invariance in control. *Automatica*, 35(11), 1747 – 1767.

Choi, S.S. and Kim, E.K. (2015). Building crack inspection using small UAV. In *2015 17th International Conference on Advanced Communication Technology (ICACT)*, 235–238.

Kada, B. and Ghazzawi, Y. (2011). Robust PID Control Design for an UAV Flight Control System. In *World Congress on Engineering and Computer Science*, volume 2.

Langson, W., Chryssochoos, I., Raković, S., and Mayne, D. (2004). Robust model predictive control using tubes. *Automatica*, 40(1), 125 – 133.

Mayne, D., Raković, S., Findeisen, R., and Allgöwer, F. (2006). Robust output feedback model predictive control of constrained linear systems. *Automatica*, 42(7), 1217 – 1222.

Mayne, D., Rawlings, J., Rao, C., and Scokaert, P. (2000). Constrained model predictive control: Stability and optimality. *Automatica*, 36(6), 789 – 814.

Mayne, D., Seron, M., and Raković, S. (2005). Robust model predictive control of constrained linear systems with bounded disturbances. *Automatica*, 41(2), 219 – 224.

McKinnon, C.D. (2015). *Data Driven, Force Based Interaction for Quadrotors*. Ph.D. thesis, University of Toronto.

Mo, R., Geng, Q., and Lu, X. (2016). Study on control method of a rotor UAV transportation with slung-load. In *2016 35th Chinese Control Conference (CCC)*, 3274–3279.

Olaru, S., De Doná, J., Seron, M., and Stoican, F. (2010). Positive invariant sets for fault tolerant multisensor control schemes. *International Journal of Control*, 83(12), 2622–2640.

Scokaert, P.O.M. and Mayne, D.Q. (1998). Min-max feedback model predictive control for constrained linear systems. *IEEE Transactions on Automatic Control*, 43(8), 1136–1142.

Tahar, K.N., Ahmad, A., and Akib, W.A.A.W.M. (2011). UAV-based stereo vision for photogrammetric survey in aerial terrain mapping. In *2011 IEEE International Conference on Computer Applications and Industrial Electronics (ICCAIE)*, 443–447.